Investigation and simulation of Double-Channel $In_{0.17}Al_{0.83}N/AlN/GaN/Al_{0.05}Ga_{0.95}N/GaN$ HEMT

Huda y. Alwajid
Department of Computer Technology Engineering, College of Information Technology, Imam Ja'afar Al-Sadiq University, Baghdad 10001, Iraq
Huda.yahya@sadiq.edu.iq

Abstract:

on this paper, a double-channel $In_{0.17}Al_{0.83}N/AlN/GaN/Al_{0.05}Ga_{0.95}N/GaN$ HEMT Investigation is done as well as comparison $In_{0.17}Al_{0.83}N/GaN$ HEMT with it and the double-channel $In_{0.17}Al_{0.83}N/GaN/Al_{0.05}Ga_{0.95}N/GaN$ HEMT. The AlN separator layer and AlGaN as back-barriers significantly enhanced the plate carrier density at the 2DEG channel, This leads to an improvement in the carrier mobility Simulation results confirm that the double-channel $In_{0.17}Al_{0.83}N/AlN/GaN/Al_{0.05}Ga_{0.95}N/GaN$ HEMT has higher drain current and transconductance.

Keyword: (HEMT, Double-channel, Transconductance, 2DEG).

I. Introduction

InAlN/GaN- based on the devices it has recently received continue to increase interest for it and are seen as strong contenders for high-power and also high-speed applications[1-3]. The lattice matched $In_xAl_{1-x}N/GaN$ HEMT (x~17%) structure It has been observed that can provide more than double the Two Dimensional-Electron-Gas (2DEG) plate carrier density ($n_s \sim 3\times10^{13} cm^{-2}$) it also helps to reduce strain-induced reliability issues [4, 5]. Furthermore, the thin barrier layers of typical InAlN/GaN devices (less than 10 nm) allow for the creation of highly scaled devices without requiring gate recesses, thereby eliminating the risk of plasma damage during the dry etching process [6]. Furthermore, the incorporation of an AlN spacer layer and AlGaN back-barriers significantly boosted the plate carrier density within the 2DEG channel, leading to enhanced carrier mobility [7].

II. Device Structure

In this section, simulation results, including drain current and transconductance characteristics for each structure, are shown. All structures are simulated using Silvaco TCAD. Simulator is calibrated according to [8]. All structures include 3nm thick intrinsic $In_{0.17}Al_{0.83}N$ as a spacer layer, a 9nm thick doped $In_{0.17}Al_{0.83}N$ (2e18) and a 3nm thick $In_{0.17}Al_{0.83}N$ as a cap layer. Additionally, the lattice constants, band gaps of different layers in all structures, and interface polarization charges of layers in the $In_{0.17}Al_{0.83}N$/GaN structure is based on [9].

A. $In_{0.17}Al_{0.83}N$ /GaN HEMT

The first structure is an $In_{0.17}Al_{0.83}N$/GaN HEMT, which includes a 15nm barrier layer of $In_{0.17}Al_{0.83}N$, a 14nm GaN layer as the main channel, a 2.5μm GaN layer as a buffer layer, and a 2μm sapphire layer as the substrate. Figure 1 (Left) the schematic desigen of cross-section of the $In_{0.17}Al_{0.83}N$/GaN HEMT is shown, while Fig. 1 (Right) depicts the conduction band. As explained in

Fig. 1 (Right), the conduction band at the interface of $In_{0.17}Al_{0.83}N$/GaN dips below the Fermi level, and forming a channel that binds carriers in the GaN channel.

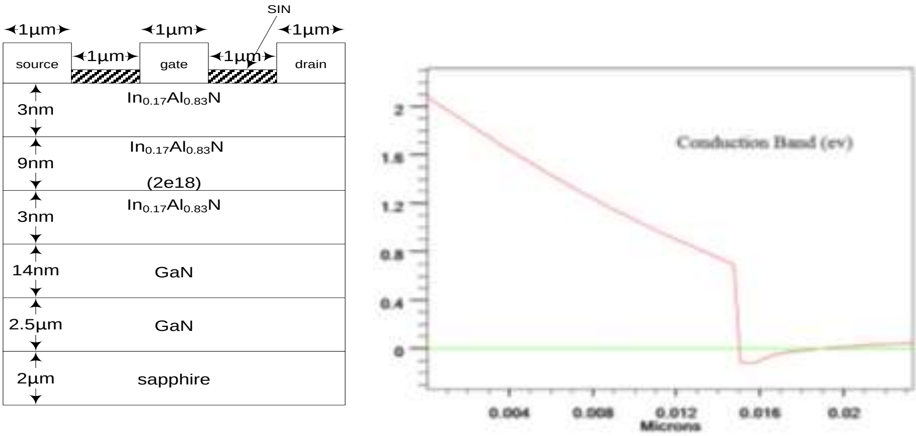

Fig. 1 (Left): Schematic; (Right): Conduction band and Fermi level of $In_{0.17}Al_{0.83}N/GaN$ HEMT.

Figure 2 depicts the drain current against drain voltage for gate voltages of 0V, -1V, -2V, and -3V.

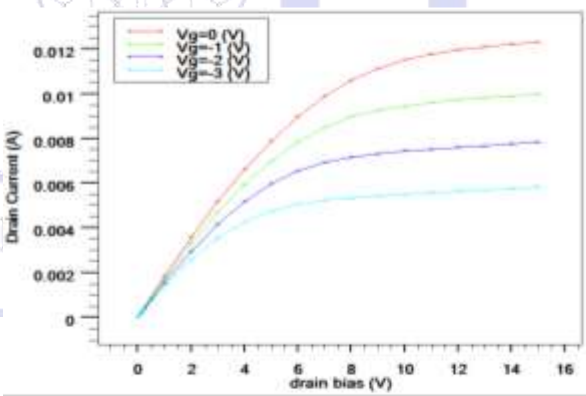

Fig. 2: I_D-V_{DS} characteristics for different V_{GS} of $In_{0.17}Al_{0.83}N/GaN$ HEMT.

Fig. 3 (Left) shows the drain current with gate voltage at V_{DS}=9V, while (Right) shows the amount of difference in transconductance with gate voltage at V_{DS}=9V. In this structure, increasing the gate voltage increases the transconductance because higher gate voltages lead to an increase in carrier density in the channel. Consequently, both the drain current and its variation increase. However, at high gate voltages, the transconductance saturates with almost no significant change.

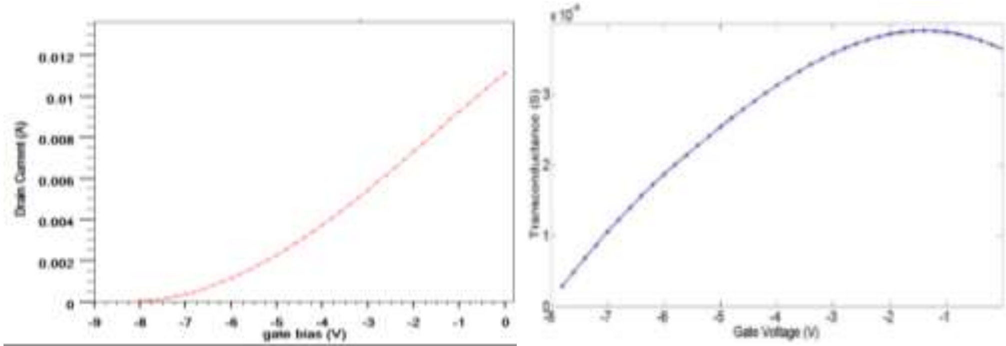

Fig. 3 (Left): I_D-V_{GS}; (Right): g_m -V_{GS} characteristic of $In_{0.17}Al_{0.83}N$/GaN HEMT at V_D=9V.

B. Double-channel $In_{0.17}Al_{0.83}N/GaN/Al_{0.05}Ga_{0.95}N$/GaN HEMT

The second structure is an $In_{0.17}Al_{0.83}N/GaN/Al_{0.05}Ga_{0.95}N$/GaN HEMT, which is formed by inserting a 21nm layer of $Al_{0.05}Ga_{0.95}N$ between the 14nm GaN channel layer and the 2.5µm GaN buffer layer. The $Al_{0.05}Ga_{0.95}N$ back barrier layer causes the formation of second channel. Fig. 4 (Left) shows a schematic cross section of the $In_{0.17}Al_{0.83}N/GaN/Al_{0.05}Ga_{0.95}N$/GaN HEMT. All simulation parameters and layer thicknesses are kept same as in $In_{0.17}Al_{0.83}N$/GaN HEMT. The only difference is the insertion a 21 nm layer of $Al_{0.05}Ga_{0.95}N$.

In this structure, the main channel is the first GaN layer, and the second GaN layer serves as a subsidiary channel. This configuration increases transconductance. In the double-channel structure, a thin layer of $Al_{0.05}Ga_{0.95}N$ is inserted at the back of the channel. The positioning of this layer is crucial, as it should be placed so that the majority of carriers remain in the GaN channel. As a result, this layer is placed 14 nm away from the interface of InAlN/GaN.

Fig. 4 (Right) shows the conduction band of the $In_{0.17}Al_{0.83}N/GaN/Al_{0.05}Ga_{0.95}N/GaN$ HEMT. As shown in the figure, the conduction band at the interface of $In_{0.17}Al_{0.83}N/GaN$ dips below Fermi level, forming a second channel that traps carriers in the GaN channel. In this structure, the $Al_{0.05}Ga_{0.95}N$ layer acts as a back barrier and contributes to the formation of the second channel.

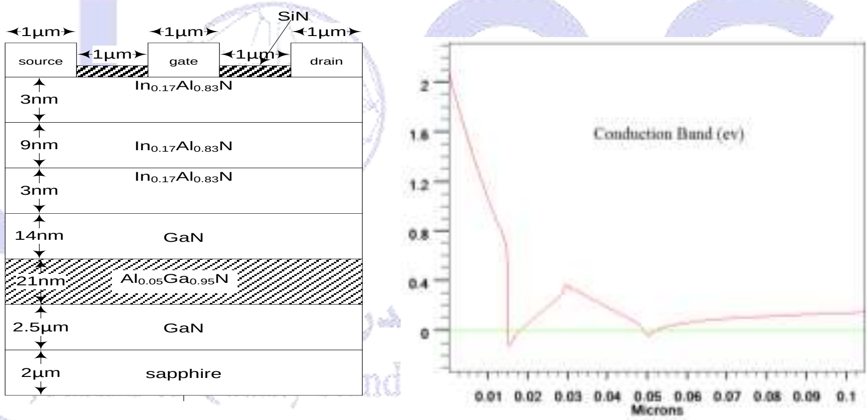

Fig. 4 (Left): Schematic; (Right): Conduction band and Fermi level of $In_{0.17}Al_{0.83}N/GaN/Al_{0.05}Ga_{0.95}N/GaN$ HEMT.

Figure 5 illustrates the drain current at gate voltages of 0V, -1V, -2V, and -3V is biased at a low drain voltage such that as a function of drain voltage.

$V_{DS}<V_{GS}-V_T$, the

When the operation of the HEMT device is in the linear region. In this region, the mobility of electrons is also linear with respect to the electric field intensity. Conversely, at high drain voltages where $V_{DS}>V_{GS}-V_T$, effective electron velocity reaches saturation and ceases to depend on the bias voltage or electric field intensity, attributed to electron collisions with the semiconductor lattice. In saturation region, electrons move with saturation velocity, and the drain current becomes independent of the drain voltage. An intense field between the gate and drain can cause an increase in gate leakage current. At high drain voltages, a resistance is created in the drain current characteristic, resulting in a small dependence of the drain current on the drain voltage.

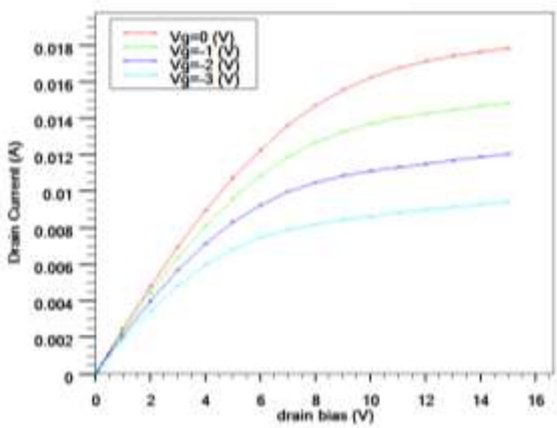

Fig. 5: I_D-V_{DS} for different V_{GS} of $In_{0.17}Al_{0.83}N/GaN/Al_{0.05}Ga_{0.95}N/GaN$ HEMT.

Fig. 6 (Left) the drain current is a show as a function of gate voltage at a drain voltage of 9V. As the gate voltage and charge density in the channel increase, the current also increases. Fig. 6 (Right) shows the variation of transconductance with gate voltage at a drain voltage of 9V. Transconductance is calculated as follows:

$$g_m = \frac{\partial I_D}{\partial V_{GS}} \qquad (1)$$

when the gate voltage is increases, the transconductance increases. The reason for this increase is that a higher gate voltage leads to a higher density of carriers in the channel, thereby increasing the current and its variations. With further increases in gate voltage, the transconductance reaches its maximum.

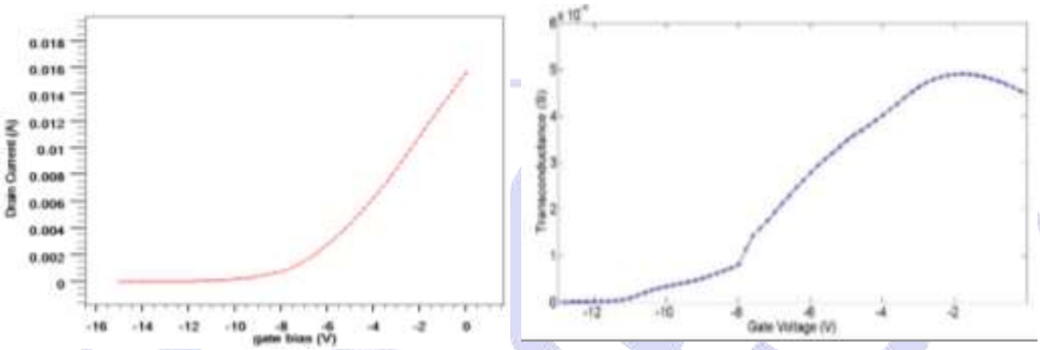

Fig. 6 (Left): I_D-V_{GS}; (Right): g_m-V_{GS} at V_{DS}=9V of $In_{0.17}Al_{0.83}N/GaN/Al_{0.05}Ga_{0.95}N/GaN$ HEMT

C. Double-channel $In_{0.17}Al_{0.83}N/AlN/GaN/Al_{0.05}Ga_{0.95}N/GaN$ HEMT

The third structure is an $In_{0.17}Al_{0.83}N/AlN/GaN/Al_{0.05}Ga_{0.95}N/GaN$ HEMT. The AlN layer has a larger band gap; therefore, the difference between the conduction bands of the AlN layer and GaN layer and the interface polarization charge increase. These factors together causes an increase in the current density and transconductance of this structure compared with the $In_{0.17}Al_{0.83}N/AlN/GaN$ HEMT. Fig. 7(Left) shows a schematic cross-sectional view of the $In_{0.17}Al_{0.83}N/AlN/GaN/Al_{0.05}Ga_{0.95}N/GaN$ HEMT. All simulation parameters and thicknesses for this structure are the same as those for the

$In_{0.17}Al_{0.83}N/GaN/Al_{0.05}Ga_{0.95}N/GaN$ HEMT. The only difference is that the 1nm spacer layer of $In_{0.17}Al_{0.83}N$ is replaced with AlN. The AlN layer has a larger band gap and polarization charge compared to the $In_{0.17}Al_{0.83}N$ spacer layer. Additionally, AlN increase the mobility of the channel. All of these factors contribute to the increase in current density and transconductance.

Fig. 7 (Right) shows the conduction band of the $In_{0.17}Al_{0.83}N/AlN/GaN/Al_{0.05}Ga_{0.95}N/GaN$ HEMT. As shown in the figure, due to high band gap of AlN layer, there is a lump in the conduction band of the barrier layer. The difference between the conduction bands of the AlN layer and the GaN layer increases, which in turn increases the current density and the transconductance.

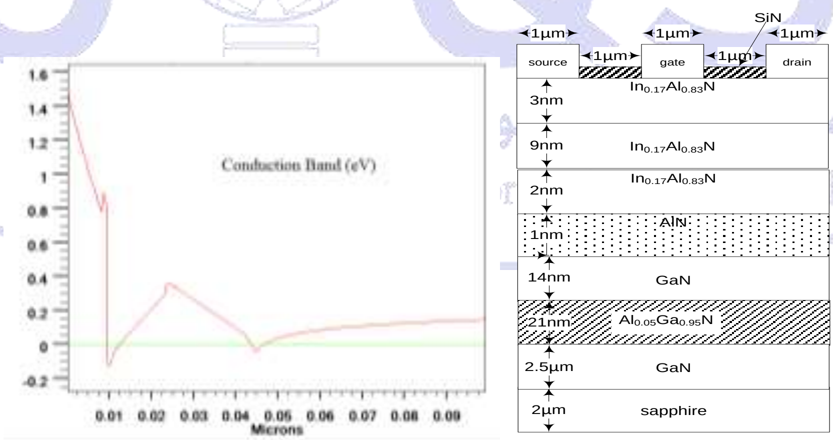

Fig. 7 (Left): Schematic; (Right): Conduction band and Fermi level of $In_{0.17}Al_{0.83}N/AlN/GaN/Al_{0.05}Ga_{0.95}N/GaN$ HEMT.

Fig. 8 shows drain current with drain voltage at gate voltage of 0V, -1V, -2V and -3V for $In_{0.17}Al_{0.83}N/AlN/GaN/Al_{0.05}Ga_{0.95}N/GaN$ HEMT. AlN layer in the spacer layer causes an increase in conduction band difference of AlN layer and GaN channel, interface polarization charge, and mobility of channel. Consequently, current density increases.

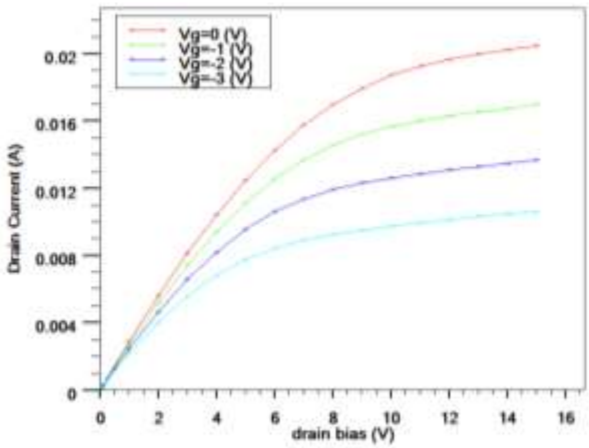

Fig. 8: I_D-V_{DS} with different V_{GS} for $In_{0.17}Al_{0.83}N/AlN/GaN/Al_{0.05}Ga_{0.95}N/GaN$ HEMT.

Fig. 9 (Left) shows the drain current as a function of gate voltage at V_{DS}=9V for the $In_{0.17}Al_{0.83}N/AlN/GaN/Al_{0.05}Ga_{0.95}N/GaN$ HEMT. As the gate voltage increases, the carrier density, and consequently the drain current, also increase. Fig. 9 (Right) shows the transconductance as a function of gate voltage at V_{DS}=9V for this structure.

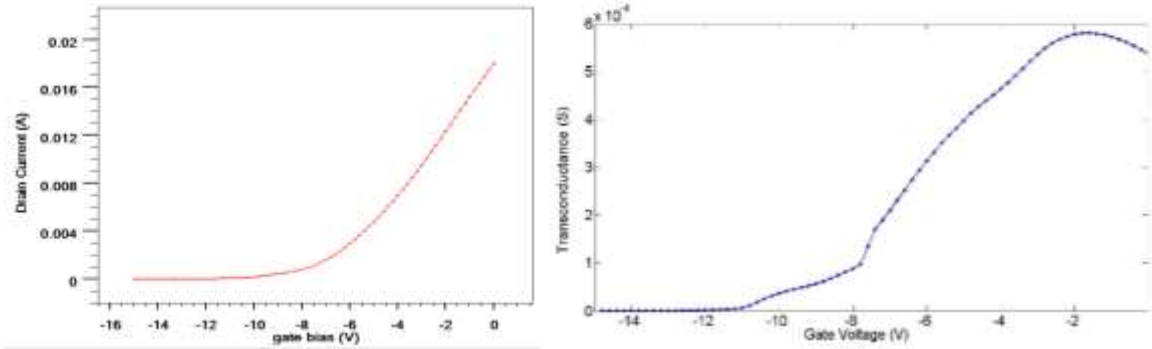

Fig. 9 (Left): I_D-V_{GS}; (Right): g_m-V_{GS} of $In_{0.17}Al_{0.83}N/AlN/GaN/Al_{0.05}Ga_{0.95}N/GaN$ HEMT at V_{DS}=9(V).

III. Comparison Results

Fig. 10 shows the variation of drain source with gate voltage at V_{DS}=15V of InAlN/GaN HEMT, InAlN/GaN/AlGaN/GaN HEMT in addition to InAlN/AlN/GaN/AlGaN/GaN HEMT. Fig.11 shows the variation of transconductance for these structures. Adding the $Al_{0.05}Ga_{0.95}N$ back-barrier layer causes the formation of a second channel, and the drain current and transconductance of the second and third structures are higher than those of the first structure, as shown in Figs. 10 and 11. Replacing the 1 nm layer of InAlN with AlN in the spacer layer enhances the conduction band gap difference between the AlN layer and the GaN channel, as well as the large interface polarization charge. This increases the drain current and transconductance of the double-channel structure with the AlN spacer layer.

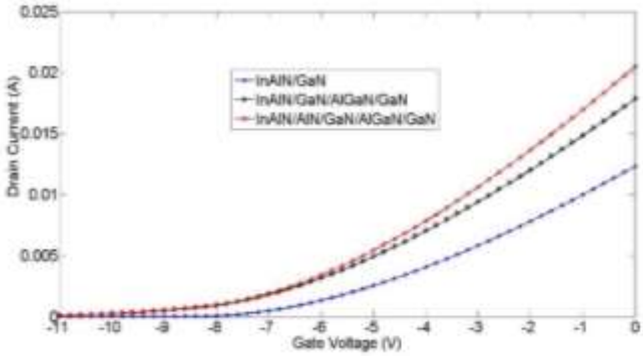

Fig. 10: Comparison of I_D-V_{GS} at V_{DS}=15V for $In_{0.17}Al_{0.83}N$/GaN, InAlN/GaN/AlGaN/GaN and InAlN/AlN/GaN/AlGaN/GaN HEMT.

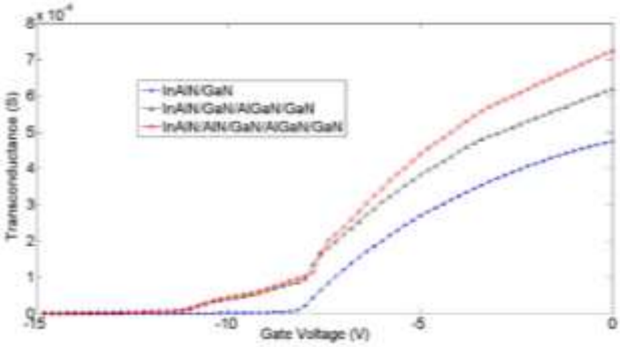

Fig. 11: Comparison of g_m-V_{GS} at V_{DS}=15V for $In_{0.17}Al_{0.83}N$/GaN, InAlN/GaN/AlGaN/GaN and InAlN/AlN/GaN/AlGaN/GaN HEMT.

V. Conclusion

InAlN/GaN heterostructures that are lattice-matched experience no strain, thereby mitigating issues related to strain-induced defect relaxation and enhancing overall reliability. In this paper, the double-channel $In_{0.17}Al_{0.83}N/AlN/GaN/Al_{0.05}Ga_{0.95}N/GaN$ HEMT is proposed and compared with $In_{0.17}Al_{0.83}N$/GaN HEMT and InAlN/GaN/AlGaN/GaN HEMT. Simulation results have shown that the drain current and transconductance of the proposed structure are higher than those of the other two structures. The presence of an AlN separator layer and also AlGaN back- barriers lead to a significant increase in the plate carrier density in the 2DEG channel, thereby enhancing carrier mobility. Consequently, the drain current and transconductance are improved for the proposed structure.

References:

[1] G. Gu et al., "Enhancement-mode InAlN/GaN MISHEMT with low gate leakage current," J. Semicond., vol. 33, no. 6, 2012, doi: 10.1088/1674-4926/33/6/064004.

[2] D. S. Lee et al., "Nanowire channel InAlN/GaN HEMTs with high linearity of g_m and f_T," IEEE Electron Device Lett., vol. 34, no. 8, pp. 969-971, 2013, doi: 10.1109/led.2013.2261913.

[3] C. Ma, G. Gu, and Y. Lü, "A high performance InAlN/GaN HEMT with low R_{on} and gate leakage," J. Semicond., vol. 37, no. 2, 2016, doi: 10.1088/1674-4926/37/2/024009.

[4] S. Arulkumaran et al., "High-frequency microwave noise characteristics of InAlN/GaN high-electron mobility transistors on Si (111) substrate," IEEE Electron Device Lett., vol. 35, no. 10, pp. 992-994, 2014, doi: 10.1109/led.2014.2343455.

[5] J. Xue et al., "Fabrication and characterization of InAlN/GaN-based double-channel high electron mobility transistors for electronic applications," Int. J. Appl. Phys., vol. 111, no. 11, 2012, doi: 10.1063/1.4729030.

[6] B. Liu et al., "An extrinsic f_{max}>100 GHz InAlN/GaN HEMT with AlGaN back barrier," J. Semicond., vol. 34, no. 4, 2013, doi: 10.1088/1674-4926/34/4/044006.

[7] P. Murugapandiyan, S. Ravimaran, and J. William, "DC and microwave characteristics of Lg 50 nm T-gate InAlN/AlN/GaN HEMT for future high power RF applications," Int. J. Electron Commun., vol. 77, pp. 163-168, 2017, doi: 10.1016/j.aeue.2017.05.004.

[8] R. Madadi, S. Marjani, R. Faez, and S. E. Hosseini, "The effect of adding InGaN interlayer on AlGaN/GaN double channel HEMT for noise improvement," J. Electr. Syst., vol. 2, no. 1, pp. 15-20, 2014.

[9] O. Ambacher et al., "Two dimensional electron gases induced by spontaneous and piezoelectric polarization in undoped and doped AlGaN/GaN heterostructures," Int. J. Appl. Phys., vol. 87, no. 1, pp. 334-344, 2000, doi: 10.1063/1.371866.